CHEMISTRY OF MATERIALS

ARTICLE

pubs.acs.org/cm

Blue Electroluminescence from Eu^{2+}-Doped GaN@SiO_2 Nanostructures Tuned to Industrial Standards

Anurag Gautam[†] and Frank C. J. M. van Veggel*[,†]

[†]Department of Chemistry, University of Victoria, Victoria, British Columbia V8W 3V6, Canada

Supporting Information

ABSTRACT: We have tuned the blue electroluminescence of surface-modified Eu^{2+}-doped GaN@SiO_2 nanoparticle to industrial standards with a peak at 450 nm and Commission Internationale de l'Eclairage (CIE−1931) coordinates of $X = 0.15$ and $Y = 0.15$. The blue electroluminescence was observed on applying a 14 V forward bias to the devices. The Eu^{2+}-doped GaN@SiO_2 nanoparticles were obtained on nitridation of Eu^{3+}-doped Ga_2O_3@SiO_2 nanoparticles at 900 °C. Subsequently, the surface of the Eu^{2+}-doped GaN@SiO_2 nanostructure was modified by reacting with dodecyletriethoxysilane at 80 °C, which enabled it to be dispersible in toluene, xylene, and benzene. Tuning of the CIE coordinates is dependent on the ratio of nitrogen to oxygen in the coordinating sphere of Eu^{2+} ions which is the origin of the blue electroluminescence.

KEYWORDS: blue electroluminescence., nanoparticles, semiconductor, Eu^{2+} ions

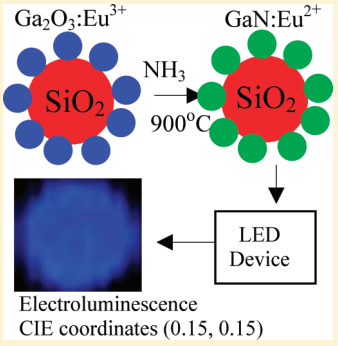

INTRODUCTION

Significant progress in solid state lighting has been achieved since the development of nitride-based blue light-emitting diodes (LEDs) from Nichia chemical industries,[1−5] but reliable and highly efficient blue LEDs are still in high demand especially polymer-based LEDs because of their cheap, flexible, and substrate suitability for daily use.[6−9] Particularly, blue-emitting materials with CIE coordinates nearly $X = 0.15$ and $Y = 0.15$ are really important as defined by the Department of Energy (DOE) and Optoelectrical Industry Development association (OIDA).[9] Blue-emitting materials are not only a major constituent for red-green-blue full color displays but also a key emitting element for generating white light. For example, combination of the GaN-based blue LED ($\lambda_{emi} \sim 465$ nm) with the $Y_3Al_5O_{12}$:Ce^{3+} yellow phosphor ($\lambda_{emi} \sim 555$ nm) gives white light.[4] Blue and UV LEDs also have great prospect in data-storage capacities in compact discs (CDs) and digital video discs (DVDs), because the storage density of compact discs is inversely proportional to the square of the laser wavelength.[2] Despite the application of organic electroluminescent devices in making blue organic light-emitting diodes (OLEDs), their low efficiency and stability still remain a challenge and calls for the use of very robust materials such as GaN.[10−13] GaN has a direct wide band gap (3.4 eV) at room temperature and is a promising host electroluminescence (EL) material for multicolor emitting phosphor. Doping of GaN thin films with Tm^{3+}, Er^{3+}, and Eu^{3+} ions results, upon excitation, in blue, green, and red emission, respectively.[14] Furthermore enhancement in the blue emission intensity was observed on doping Tm^{3+} in $Al_1Ga_{1-X}N$ instead of GaN thin film. The CIE coordinates were tuned to $X = 0.13$, $Y = 0.09$, and the enhanced emission from Tm^{3+} ions was proportional to the Al content in the film.[15] Recently, Yang et al.[16] fabricated GaN-based blue LEDs with an EL peak centered at 447 nm. In another report Zhao et al.[17] obtained blue EL by using Au/AlN/p-Si heterostructure and had an EL peak centered at 490 nm. The CIE coordinates are $X = 0.25$, $Y = 0.33$, as calculated by us, which show a deviation from the blue region.

ZnO based heterostructures were also applied in the fabrication of EL devices. The blue EL emission from n-ZnO/n-$Mg_yZn_{1-y}O$/$Zn_{1-x}Cd_xO$/P-SiC heterojunction diodes as reported by Nakamura et al.[18] has an EL peak centered at 480 nm. The CIE coordinates, as calculated by us, are $X = 0.29$, $Y = 0.32$, which is away from the required blue. Li et al.[6] also fabricated a blue EL device using ZnO based heterojunction diodes in the presence of active layer of CdZnO with an El peak centered at 459 nm. Although the peak centered in the blue, the CIE coordinates, as calculated by us, are $X = 0.62$, $Y = 0.32$, again away from blue. Ultraviolet-blue LEDs device fabricated by Guo et al.[19] used ZnO nanowires/polymer/p-GaN in heterojunction structure with the EL emission peaks were at 400 nm. The CIE coordinates, as calculated by us, are $X = 0.62$, $Y = 0.23$ and are not in the region of the desired blue.

However, so far GaN-based devices fabricated are mostly thin film based grown by metalorganic chemical vapor deposition (MOCVD) or molecular beam epitaxy (MBE). The main disadvantages of the films are their poor mechanical properties, which prevent them from convenient fabrication into desired shapes and their high cost of production. On the other hand, nano powder-based GaN synthesis are cheap and relatively simple processes compare to the film based devices, which makes

Received: July 25, 2011
Revised: September 14, 2011
Published: October 04, 2011

nanopowders attractive for fabrication of (polymer-based) devices. Despite huge progress in GaN technology only a few papers have studied the optical properties of solution-based synthesis of GaN nanoparticles.[20]

Recently, blue emission proof of principle was achieved by our group. We fabricated blue EL devices by coating Eu^{2+}-doped GaN nanoparticles on 50 nm SiO_2 nanoparticles with the EL emission peak centered at 485 nm.[21] The Eu^{2+}-doped GaN@SiO_2 nanocomposites exhibited blue emission when excited in the ultraviolet region with the CIE coordinates $X = 0.18$ and $Y = 0.23$, which are well within the blue region but not ideal. The Eu^{2+}-doped GaN@SiO_2 nanocomposite materials were synthesized via a simple solid state reaction. The strategy applied to grow a shell of Eu^{3+}-doped Ga_2O_3 on the surface of 50 nm silica bead followed by nitridation in a flow of NH_3 at 900 ^oC, resulted in Eu^{2+}-doped GaN@SiO_2 nanoparticles. We also provided evidence that the Eu^{2+} is likely located at the GaN-SiO_2 interface. We also fabricated blue EL devices with InN@SiO_2 nanoparticles with an EL peak at 460 nm and had CIE coordinates of ($X = 0.18$, $Y = 0.23$) which fall well in the blue region of the spectrum but, again, are not ideal.[22] Although blue EL emission has been achieved, three industrial demands further motivated us to optimize from these encouraging results, which are as follows:

(i) Reduction in disruption of the active layers thickness (typically 100 nm thick) of Eu^{2+}-doped GaN@SiO_2 nanoparticles by coating Eu^{2+}-doped GaN on much smaller SiO_2 nanoparticles,

(ii) Tuning of CIE coordinates to ($X \leq 0.15$ and $Y \leq 0.15$) to the required industrial standard,[9]

(iii) Dispersion of Eu^{2+}-doped GaN@SiO_2 nanoparticles in toluene, xylene, and benzene. A dispersion in toluene or xylene will facilitate the industrial processing of LEDs, because many polymers are spin coated from toluene and xylene solutions.

In this article we adapted our strategy, i.e. a shell of Eu^{3+}-doped Ga_2O_3 was grown on the surface of 15 nm silica bead and reduced to Eu^{2+}-GaN@SiO_2 nanoparticles during nitridation. The allowed $4f^65d^1 \rightarrow 4f^7$ electronic transition of Eu^{2+} ions permits one to tailor the luminescence of the Eu^{2+}-doped GaN@SiO_2 nanoparticles by subtle change of the crystal field, which is a clear advantage over other lanthanides, i.e. in their Ln^{3+} oxidation state.

The resulting Eu^{2+}-doped GaN@SiO_2 nanoparticles were applied to fabricate EL devices after treatment with dodecyletriethoxysilane ($C_{12}H_{25}Si(OC_2H_5)_3$, DTES), which enabled the nanoparticles to be dispersible in toluene, xylene, and benzene. The Eu^{2+}-doped GaN@SiO_2 nanoparticles were characterized with Transmission Electron Microscopic (TEM), Energy Dispersive X-ray spectroscopy (EDS), X-ray Diffraction (XRD) analysis, Fourier Transform Infrared (IR) analysis, Electron Paramagnetic Resonance (EPR) measurement, Photoluminescence (PL), and EL analyses of fabricated LEDs.

RESULTS AND DISCUSSION

Optical Characterization of Eu^{2+}-Doped GaN@SiO_2 Nanoparticles. SiO_2 nanoparticles of 15 nm in size were synthesized by using a ternary microemulsion system,[23] by hydrolysis and condensation of tetraethyl orthosilicate in the presence of Igepal CA-520 as surfactant. A thin layer of Eu^{3+}-doped gallium hydroxide was then grown on the silica surface by using a urea-based homogeneous precipitation reaction.[21] These Eu^{3+}-doped gallium hydroxide nanoparticles were converted to gallium oxide by annealing at 800−900 ^oC in air for 2 h, which resulted in Eu^{3+}-doped Ga_2O_3@SiO_2 nanoparticles. Finally, Eu^{3+}-doped Ga_2O_3@SiO_2 nanoparticles were converted to Eu^{2+}-doped GaN@SiO_2 nanoparticles in a flow of NH_3 at 900 ^oC for 3 h. A color change of nanocomposites from white to yellow was observed as expected for the formation of GaN. The overall reaction equation of the nitridation is shown below

$$Ga_2O_3(s) + 2NH_3(g) \rightarrow 2GaN(s) + 3H_2O(g)$$

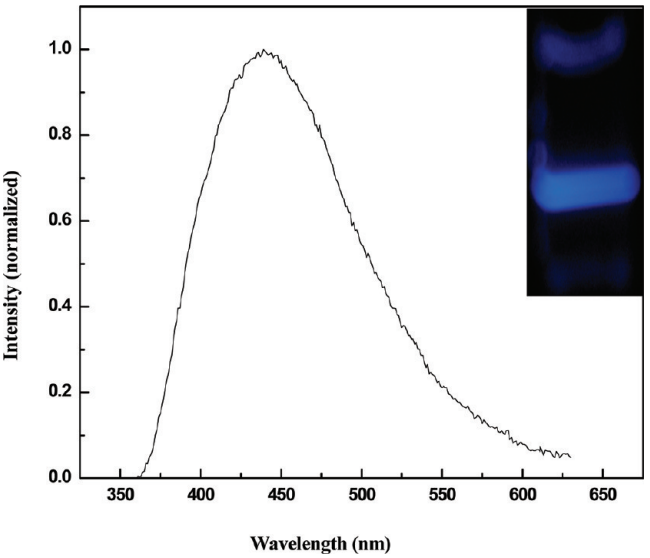

Figure 1. The photoluminescence spectrum of DTES-treated Eu^{2+}-doped GaN@SiO_2 nanoparticles after dispersing in toluene. The inset shows the digital photograph of dispersed Eu^{2+}-doped GaN@SiO_2 nanocomposite, photograph taken at 90 degree to exciting light. Exciting with He−Cd laser operating at 325 nm.

Subsequently, the nanoparticles were treated with dodecyletriethoxysilane (DTES) at 80 ^oC for 24 h.[24] The Eu^{2+}-doped GaN@SiO_2 DTES-treated was dispersed in toluene. Figure 1 shows the photoluminescence (PL) spectrum of nanoparticles dispersed in toluene on exciting with a He−Cd laser operating at 325 nm. The PL spectrum shows a blue emission peak centered at 442 nm, and the inset shows a digital photograph of the dispersed nanoparticles in toluene.

The origin of this emission is due to the presence of the Eu^{2+} ion at the interface of GaN and SiO_2 nanoparticles.[21] The PL spectrum of Eu^{2+}-doped GaN@SiO_2 nanoparticles does not show any characteristic luminescence of Eu^{3+} ions. The excitation spectrum (Figure S1) supports the fact that energy transfer from excited GaN to Eu^{2+} occurs. The PL spectrum of Eu^{3+}-doped Ga_2O_3@SiO_2 nanoparticles (Supporting Information Figure S1) shows the Eu^{3+}-based PL peaks between 580 to 650 nm together with a weaker defect related PL of Ga_2O_3 at 425 nm.[25] The bare SiO_2 nanoparticles have a very weak PL peak at 412 nm (Supporting Information Figure S1) in agreement with the value reported for silica.[26] GaN nanoparticles also show a very weak PL peak at 395 nm, which is probably a band edge emission (Supporting Information Figure S1) in agreement with previous results obtained by our group.[27−29] Furthermore, the Eu^{3+} ions emission lines were also observed in Eu^{3+}-doped Ga_2O_3@SiO_2 nanoparticles in between 580 to 650 nm upon excitation with λ_{exi} = 464 nm (i.e., direct excitation of the Eu^{3+} ions). After nitridation

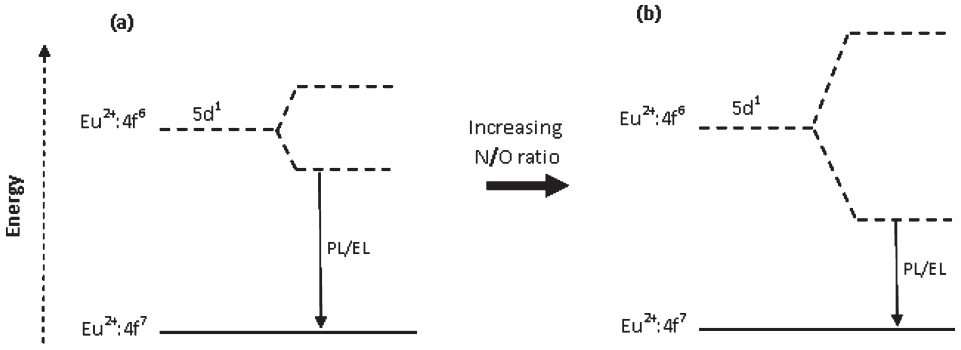

Figure 2. Schematic splitting of 5d orbital of Eu^{2+} in Eu^{2+}-doped GaN@SiO_2 nanoparticles (a) in general condition and (b) in nitrogen-rich environment.

Eu^{2+}-doped Ga_N@SiO_2 nanoparticles lacked the presence of any Eu^{3+} based emission, which further support the reduction of Eu^{3+} ions to Eu^{2+} ions (Supporting Information Figure S2).

The position of emission peak of the Eu^{2+} ions strongly relies on the environment (i.e., on the crystal field). So, the tailoring of the spectrum depends on the ratio of nitrogen and oxygen in the coordinating sphere. The nitrogen-rich surrounding of the Eu^{2+} ions redshifts the emission peak (Supporting Information Table S1). The higher formal charge of the N^{3-} compared to O^{2-} ions and lower electronegativity of nitrogen (3.04) compared to oxygen (3.44) causes a larger ligand-field splitting of 5d levels (4f levels remain largely unaffected), which lowers the energy of lower lying 5d level more in nitrogen rich condition.[30] This is represented schematically in the diagram in Figure 2. The larger splitting of the 5d orbital in a nitrogen-rich environment is shown in Figure 2b, where its energy is further lowered with respect to its energy in Figure 2a (the general case), conversely shift the emission spectrum toward longer wavelength. The coordinates were tuned with respect to our earlier result[21] by carefully controlling the synthesis conditions. The compositional analysis of Eu^{2+}-doped GaN@SiO_2 nanoparticles were studied by Energy Dispersive X-ray spectroscopy (EDS). The Eu^{2+}-doped GaN@SiO_2 data show the presence of Si, Ga, Eu, O, and N (Supporting Information Figure S3). The atomic ratio of Ga to N is 1:1. So the sample is in stoichiometric ratios as required for GaN. It is observed (Supporting Information Table S1) that the increasing N/O ratio causes a redshift of the emission spectrum, which is in agreement with the larger crystal field splitting in nitrogen rich condition.

The presence of Eu^{2+} ions in Eu^{2+}-doped GaN@SiO_2 was further confirmed by the lifetime decay curve of the excited Eu^{2+} ions (Supporting Information in Figure S4). The measured lifetimes are 1.73 μs (80%) and 6.0 μs (20%) for the emission at 450 nm (λ_{exi} = 355 nm) are in the agreement with the lifetime of Eu^{2+} ions.[21] Furthermore definite proof of the presence of Eu^{2+} in the europium-doped GaN@SiO_2 nanoparticles was obtained by EPR analysis (Supporting Information Figure S5). The EPR spectrum confirmed the presence of Eu^{2+} in the europium-doped GaN@SiO_2 nanocomposites. The observed spectrum is similar to that obtained for the Eu^{2+}-doped heavy metal fluoride glasses (ZBLAN).[31]

EL devices were fabricated with the configuration of ITO||PEDOT:PSS||DTES-treated Eu^{2+}-doped GaN@SiO_2||Ca||Al. In brief, poly(3,4-ethelenedioxythiophene) doped with poly(styrene sulfonic acid) (PEDOT:PSS) was spin coated on a cleaned indium tin oxide (ITO) glass substrate and then dried at 110 °C in vacuum. Subsequently, DTES-treated Eu^{2+}-doped GaN@SiO_2 nanoparticles dispersed in toluene were spin coated on top of the

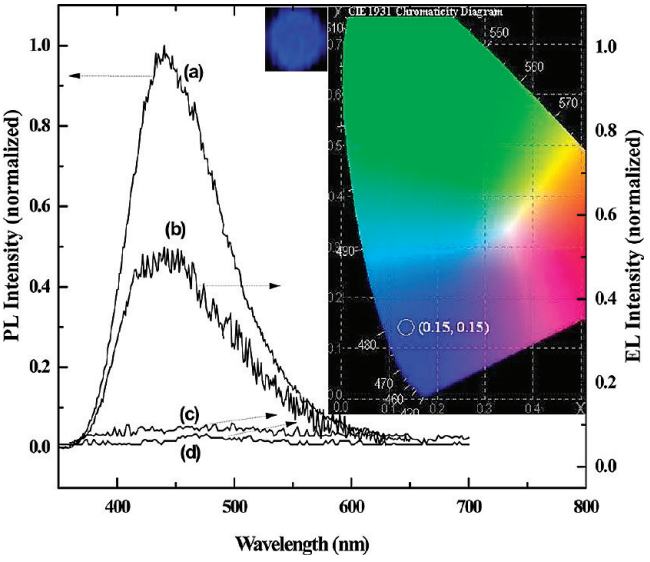

Figure 3. (a) PL spectrum of Eu^{2+}-doped GaN@SiO_2 nanoparticles, (b) EL spectrum collected from an ITO||PEDOT:PSS||Eu^{2+}-doped GaN@SiO_2 (after reacting with DTES)||Ca||Al devices, (c) EL spectrum collected from ITO||PEDOT:PSS||Eu^{3+}-doped Ga_2O_3@SiO_2||Ca||Al, and (d) EL spectrum collected from ITO||PEDOT:PSS||GaN@SiO_2||Ca||Al devices. The inset shows digital picture of EL emission from devices together with its position in CIE chromaticity diagram of 1931.

PEDOT:PSS layers and dried in vacuum at 65 °C for overnight. Subsequently, the metallic cathode (20 nm thick Ca and 150 nm Al) was thermally evaporated onto the nanocomposite layer at 5×10^{-5} Torr using a shadow mask to complete the device. The devices have an active area of ~7.5 mm^2. On applying a 14 V forward bias to the device, a blue emission was observed with the naked eye, and the EL emission spectrum was recorded. Figure 3 (a),(b) compares the PL emission of Eu^{2+}-doped GaN@SiO_2 nanoparticles with the EL emission of the device fabricated using Eu^{2+}-doped GaN@SiO_2 nanocomposites. EL emission peak is centered at 450 nm. We reproduced this EL spectrum 3 times from this device having active area ~7.5 mm^2. We did not observe any Joule heating effect in the EL spectrum. The calculated CIE coordinates were $X = 0.15$ and $Y = 0.15$, which fall well within the blue region of the 1931 CIE diagram as shown in Figure 3. The CIE coordinates are in the ideal range for a blue color as defined by the Department of Energy (DOE) and Optoelectrical Industry Development association (OIDA).[9] We also observed the blue

dx.doi.org/10.1021/cm202139u |*Chem. Mater.* 2011, 23, 4817–4823

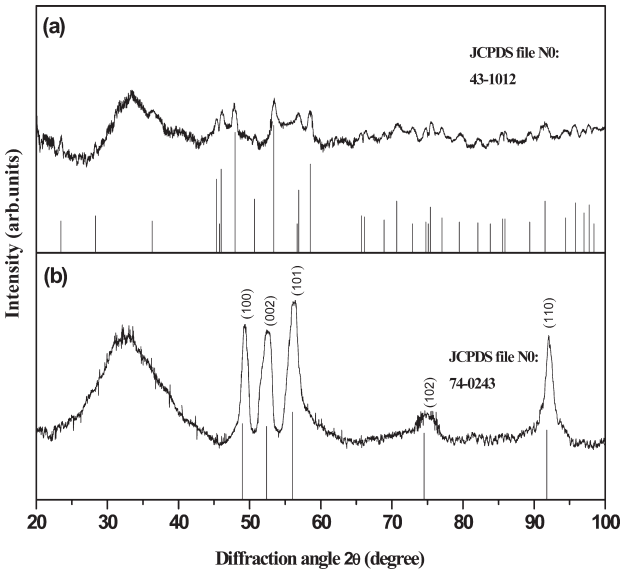

Figure 4. XRD pattern of (a) Eu^{3+}-doped Ga_2O_3@SiO_2 and (b) Eu^{2+}-doped GaN@SiO_2 after reacting with DTES at 85 °C for 24 h. The sticks are the peaks from the JCPDS reference spectrum.

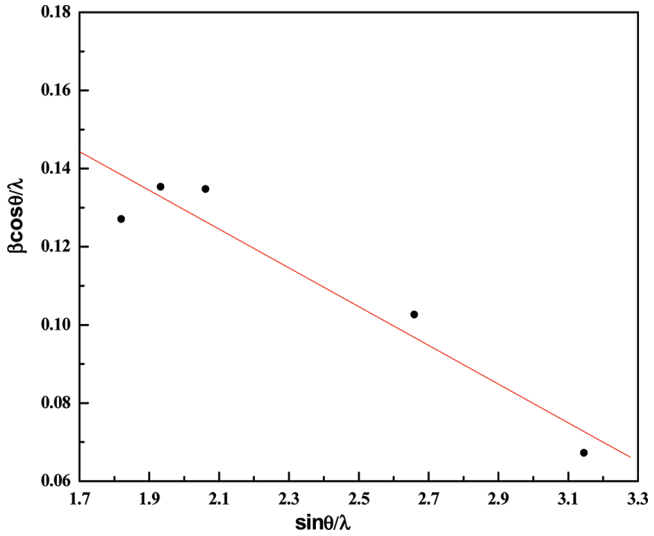

Figure 5. $\beta\cos\theta/\lambda$ vs $\sin\theta/\lambda$ for Eu^{2+}-doped GaN@SiO_2 after reacting with DTES at 85 °C for 24 h. The symbol (●) shows the experimental data points, and the red line is the least-squares fit through the data.

EL by the naked eyes from samples 1−3 shown in (Supporting Information Table S1). Sample 4 was not used in fabrication of devices, because their CIE coordinates were not in the desired region. Control experiments were also performed under the identical conditions using the Eu^{3+}-doped Ga_2O_3@SiO_2 and GaN@SiO_2 nanocomposites after treatment with DTES; they did not show EL, as shown in Figure 3c,d, respectively. This evidence supports the fact that the blue EL originates from the Eu^{2+} ions doped in GaN@SiO_2 nanocomposites.

X-ray Diffraction and Morphological Analysis. Figure 4a shows the nanomaterials used for the nitridation, confirming the presence of Ga_2O_3. Figure 4b shows the XRD pattern of DTES-treated Eu^{2+}-doped GaN@SiO_2 nanoparticles, consistent with a complete conversion of the oxide to the nitride. The XRD reveals the hexagonal wurtzite structure of GaN. The diffraction peak appears at 2θ angles of 49.3, 52.5, 56.3, 74.9, and 92.0 degrees are assigned to be diffraction from (100), (002), (101), (102), and (110) crystals planes, respectively (JCPDS Card, file No. 74-0243).[32] The average crystallite size was 8.0 nm calculated by applying the Scherrer equation as given below

$$t = 0.9\lambda/\beta\cos\theta_\beta$$

where t is the crystallite size, λ is the wavelength of the X-ray, β is full width at half maxima (fwhm), and θ is the Bragg angle.

The lattice parameters of GaN are a = 0.3176 and c = 0.51644 nm and agree well with the reported bulk value of GaN crystals.[32] They were calculated by applying the formula of hexagonal d-spacing as given below[33]

$$\frac{1}{d^2} = \frac{4}{3}\frac{(h^2 + hk + k^2)}{a^2} + \frac{l^2}{c^2}$$

where d is the distance between the adjacent planes in the set of (h k l).

The calculated density of GaN in as-prepared nanocomposites is 6.16 g/cm^3, which is close to the value of bulk GaN (6.15 g/cm^3).[32] The broad hump at the 2θ angle of 33 degrees is from amorphous silica. There is no evidence of the presence of any remaining Ga_2O_3 which confirms complete conversion of Ga_2O_3 on the silica surface to GaN during nitridation. The full-width at half maxima (fwhm) can be expressed as a linear combination of the contribution from the lattice strain and crystallite size. The effect of the strain and particle size on the fwhm can be expressed by the following equation[34]

$$\frac{\beta\cos\theta}{\lambda} = \frac{1}{\varepsilon} + \frac{\eta\sin\theta}{\lambda}$$

where θ is the Bragg diffraction angle of the peak, ε is the effective crystallite size, and η is the effective strain. Figure 5 shows a plot of $\beta\cos\theta/\lambda$ vs $\sin\theta/\lambda$ for Eu^{2+}-doped GaN@SiO_2 nanoparticles. The slope of the fitted line is negative indicating a compressive strain in Eu^{2+}-doped GaN@SiO_2 nanoparticles. The effective crystallite size that takes strain into account can be estimated from the intercept of the fitted line shown in the Figure 5. The crystallite size obtained was 7.0 nm, which compares well with the value calculated from Scherrer's equation.

The SEM micrograph of Eu^{2+}-doped GaN@SiO_2 nanoparticles is shown in Figure S6. The Eu^{2+}-doped GaN@SiO_2 nanoparticles is 20 ± 2 nm, as is clearly visible in the micrograph and the size SiO_2 nanoparticles is 15 ± 2 nm. So, as analyzed by SEM micrograph, the size of *the GaN nanoparticles coated on SiO_2 surface* are 5 nm in size, i.e. the GaN is not present as a thin shell, which is in excellent agreement with the result obtained by XRD. The TEM micrograph of Eu^{2+}-doped GaN@SiO_2 nanocomposites is shown in Figure 6a and DTES-treated Eu^{2+}-doped GaN@SiO_2 nanocomposites is shown in Figure 6b. The small dark GaN nanoparticles coated on the bigger SiO_2 nanoparticles have a size of 3−5 nm. This result is in good agreement with the results obtained by XRD and SEM studied. The coating of GaN nanoparticle on silica is nonhomogeneous due to the lattice mismatch between SiO_2 and GaN nanoparticles.[21] It is noted that the TEM image of the Eu^{3+}-doped Ga_2O_3@SiO_2 (Figure 6c) has the Ga_2O_3 as very small nanoparticles adhered to the SiO_2 bead, which is in contrast with previous results, but likely due to the larger curvature of the beads used in the current study giving a higher surface energy.[21]

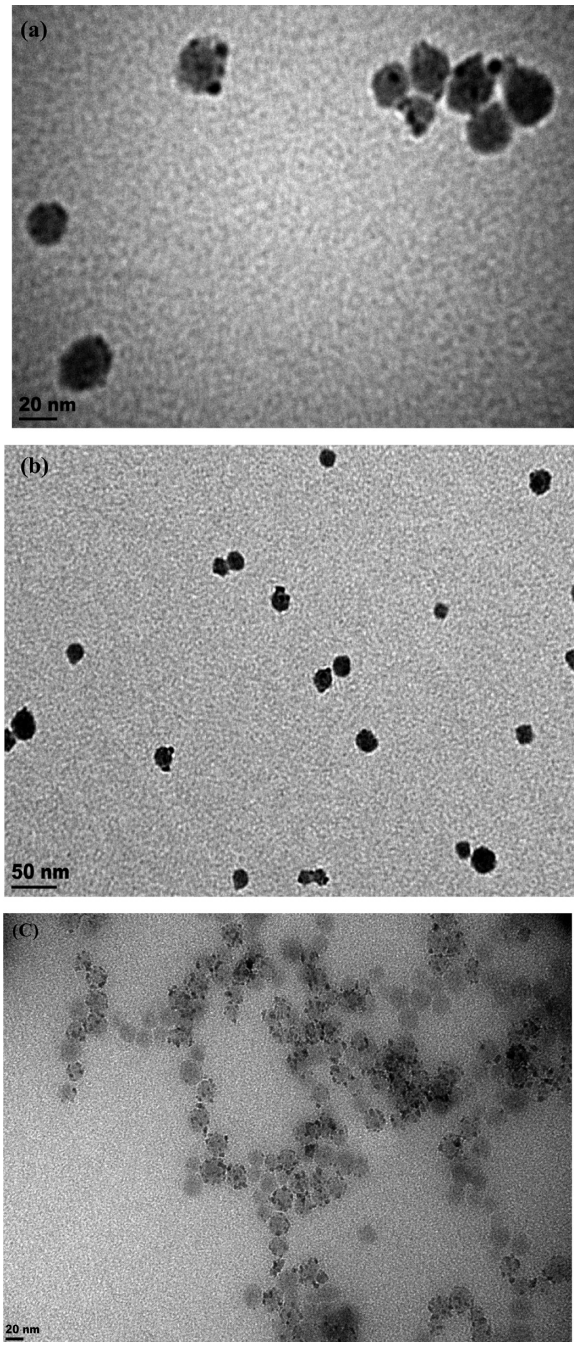

Figure 6. TEM micrographs of (a) Eu^{2+}-doped GaN@SiO_2, (b) DTES-treated Eu^{2+}-doped GaN@SiO_2, and (c) Eu^{3+}-doped Ga_2O_3@-SiO_2 nanocomposites.

The Raman spectrum of Eu^{2+}-doped GaN@SiO_2 is shown in Figure 7a. The formation of GaN was confirmed by the spectrum which shows the allowed E_2 (high) phonon at 570 cm^{-1} and A_1 [longitudinal optical (LO)] phonon at 734 cm^{-1}.[35] The strong E_2 (high) phonon line reflects the characteristic of the hexagonal crystalline phase of GaN, as obtained by XRD. The peak near 420 cm^{-1} is ascribed to acoustic overtones, in accordance with the previous results.[36] The Raman spectrum of DTES-treated Eu^{2+}-doped GaN@SiO_2 nanocomposites (Figure 7b) shows an additional peak at 650 cm^{-1} which is assigned to the symmetrical SiO_3 stretching frequency of DTES in agreement with surface

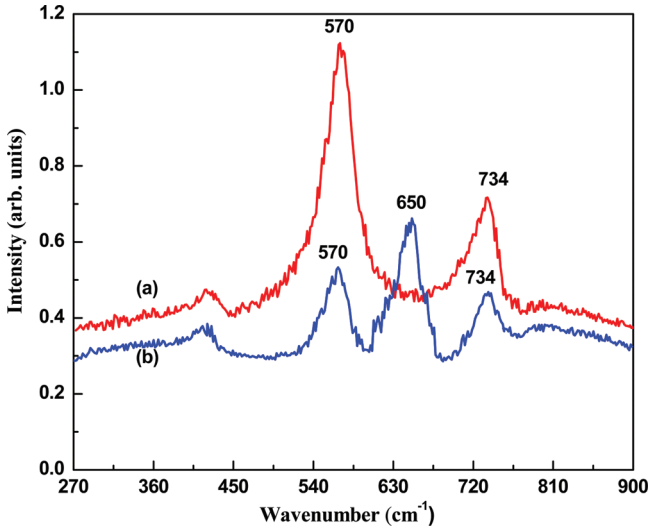

Figure 7. Raman spectrum of (a) Eu^{2+}-doped GaN@SiO_2 obtained after nitridation at 900 °C for 3 h in ammonia and (b) Raman spectrum of DTES-treated Eu^{2+}-doped GaN@SiO_2 nanocomposites.

bonded O_3Si-R groups.[37] Furthermore the broad peaks between 270 and 450 cm^{-1} are assigned as a network bending mode of Si−O−Si vibration of SiO_2 nanoparticles.[38,39] Figure S7 shows the IR spectrum of DTES-treated Eu^{2+}-doped GaN@SiO_2 nanocomposites. The vibrational peak extended over the range of 550−750 cm^{-1} is assigned to GaN which is also present in untreated Eu^{2+}-doped GaN@SiO_2 nanocomposites. DTES-treated Eu^{2+}-doped GaN@SiO_2 nanocomposites show additional vibrational peaks at 2976 and 2855 cm^{-1} which are characteristic of the $-CH_3$ asymmetric and symmetric stretching vibrations in DTES. Furthermore, the vibrational peak at 2925 cm^{-1} (Supporting Information Figure S7c) is assigned to asymmetric vibration of $-CH_2$ group in DTES,[22] and the peaks at 792 cm^{-1}, 957 cm^{-1}, 1390 cm^{-1}, and 1467 cm^{-1} are in agreement with the vibrational peaks of DTES as observed in pure DTES.

CONCLUSIONS

In conclusion, blue EL devices were fabricated with DTES-treated Eu^{2+}-doped GaN@SiO_2 nanoparticles with an EL emission peak at 450 nm. The EL emission from Eu^{2+}-doped GaN@SiO_2 nanoparticles has been tuned to the CIE coordinates of $X = 0.15$ and $Y = 0.15$, as required by the industrial standard defined by DOE and OIDA. This result was obtained by controlling the ratio of nitrogen and oxygen in the coordinating sphere of Eu^{2+} ions. Eu^{2+}-doped GaN@SiO_2 nanoparticles are dispersible in toluene, xylene, and benzene after reacting then with DTES. The fabrication method of Eu^{2+}-doped GaN@SiO_2 nanocrystal-based EL device described here may provide a convenient and cheap choice to produce blue light-emitting devices.

EXPERIMENTAL DETAILS

Chemicals used are tetraethyl orthosilicate (TEOS), aqueous ammonium hydroxide (28−30%), gallium nitrate (99.98%), europium nitrate (99.99%), methylmethacrylate, urea, potassium bromide, ethanol (99.9%), and dodecyletriethoxysilane ($C_{12}H_{25}Si(OC_2H_5)_3$, DTES) and were used as received from Sigma-Aldrich. The anhydrous ammonia gas

dx.doi.org/10.1021/cm202139u |*Chem. Mater.* 2011, 23, 4817–4823

(99.999%) used for the nitridation was purchased from Praxair. Distilled water is used in the experiments.

Preparation of Bare Silica Nanoparticles. In a typical microemulsion for preparation of silica nanoparticles using a ternary microemulsion system,[23] 0.1 M surfactant (Igepal CA-520 from Sigma-Aldrich) was dissolved in 10 mL of cyclohexane, followed by addition of 0.09 mL of water, 0.1 mL of TEOS, and 0.060 mL of NH_4OH. The reaction was allowed to stir for 24 h followed by addition of ethanol to break the microemulsion and recover the particles. The particles were washed a couple of times with ethanol, and finally it is washed with distilled water. The average size of the SiO_2 nanoparticles obtained was 15 ± 2 nm, based on the average of 100 nanoparticles.

Preparation of Eu^{3+} (5%)-Doped Ga_2O_3@SiO_2 Nanocomposites. A previously reported[21] method was used here for synthesis of Eu^{3+}-doped Ga_2O_3@SiO_2 with slightly modification. Briefly, 0.6 g of urea was dissolved in water and added to a flask containing 15 mL of 15 nm silica nanoparticles. Then an aqueous solution of $Ga(NO_3)_3$ and $Eu(NO_3)_3$ was added dropwise to the flask, and the solution was vigorously stirred at 85 °C. After 3 h the mixture of the solution resulted in a white precipitate. This precipitate was purified 3 times in water by centrifugation and redispersion. This purified precipitate was dried in vacuum. Finally, it was annealed at 800−900 °C for 2 h.

Preparation of Eu^{2+}(5%)-Doped GaN@SiO_2 Nanoparticles. For sample 2 in Table S1 we did the following: approximately 100 mg of Eu^{3+}-doped Ga_2O_3@SiO_2 nanoparticles was put in a quartz crucible, and then the crucible was placed in the middle of an electric furnace (Lindberg/Blue, Model Name: Tube Furnace). The furnace was heated to 900 °C for 3 h in NH_3 atmosphere at a rate of 5 °C min^{-1}. Furthermore, the sample was left at 900 °C for 3 h before it was cooled down to room temperature in NH_3 atmosphere at a rate of 5 °C min^{-1}. The ammonia flow was maintained at 10 sccm (standard cubic centimeter per minute at STP). The color of the sample changed from white to yellow during the nitridation process. Finally, Eu^{2+}-doped GaN@SiO_2 nanoparticles was then reacted with dodecyletriethoxysilane ($C_{12}H_{25}Si(OC_2H_5)_3$, DTES) at 85 °C for 24 h. The mixture was then filtered. After filtration the DTES-treated Eu^{2+}-doped GaN@SiO_2 was dried in vacuum at 65 °C. For the other three samples in Table S1 we used the following: sample 1, the flow of ammonia was changed to argon in the cooling phase; sample 3, the heating phase and reaction time at 900 °C were both 3.5 h; sample 4, as sample 3, but cooled under an argon atmosphere.

Fabrication of Electroluminescence (EL) Device Using DTES-Treated Eu^{2+}-DopedGaN@SiO_2 Nanoparticles. Devices with a configuration of ITO||PEDOT:PSS||DTES-treated Eu^{2+}-doped GaN@SiO_2||Ca||Al were fabricated as follows. First, poly(3,4-ethelenedioxythiophene) doped with poly(styrene sulfonic acid) (PEDOT:PSS) was spin coated on a cleaned indium tin oxide (ITO) glass substrate and then dried at 110 °C in vacuum. Subsequently, DTES-treated Eu^{2+}-doped GaN@SiO_2 nanoparticles dispersed in toluene, and the mixture was sonicated for 6 h. After sonication the nanoparticles were spin coated on top of the PEDOT:PSS layers substrate at 1500 rpm for 30 s under air-free conditions. The resulting film was then dried in a vacuum at 65 °C for overnight. Finally, the metal cathode (20 nm thick Ca and 150 nm Al) was thermally evaporated onto the nanocomposite layer at 5×10^{-5} Torr using a shadow mask to complete the device. The devices having an active area of ~7.5 mm^2. On applying a direct current (dc) of 14 V to the device with the positive terminal connected to the ITO electrode and the negative terminal to calcium protected cathode layers, the blue emission was observed in forward bias with the naked eye, and the EL emission spectrum was recorded. The EL was characterized using the Edinburgh Instruments' FLS 920 fluorescence spectrometer (vide supra).

X-ray Diffraction Analysis. Approximately 40−50 mg of a sample was placed onto a zero-diffraction quartz plate using ethanol. The X-ray diffraction data were collected over a range of $2\theta = 20-140$ degree. XRD patterns were measured with Cr (30 kV, 15 mA) radiation on a Rigaku Miniflex diffractometer with variable divergence slit, 4.2° scattering slit, and 0.3 mm receiving slit. The scanning step size was 0.5° per minutes.

Transmission Electron Microscopic (TEM) Measurements. A JEOL JEM-1400 tungsten filament up to 80 kV Transmission Electron Microscope was used to collect the TEM images. TEM specimens were prepared by dipping a copper grid (600 mesh) which was coated with an amorphous carbon film into the ethanol dispersion of the nanomaterials composites, followed by drying at room temperature.

Photoluminescence (PL) Measurements. Room temperature PL measurements of all samples (in EPR tube) were performed using a 325 nm Omnichrome Series 74 He−Cd laser by Melles Griot, using a band-pass filter. For all the measurements, the detector employed was an R928P Hamamatsu PMT, and the resolution due to the slits aperture was 1 nm. The laser beam was focused on the Eu^{2+}-doped GaN@SiO_2 nanoparticles through the microscope. A SpectroPro-500 monochromator by Acton Research Corporation was used to scan the PL signal in the visible range (350−750 nm). The signal was amplified by a differential preamplifier and then acquired by the computer. The lifetime of the Eu^{2+} ion was collected by exciting with the 355 nm (Vibrant tunable laser system, model 355 IIb) harmonic line of a Quantel Nd:YAG nanosecond laser. The lifetime decays were fitted by two-exponentials based on the following equation[21]

$$\frac{I(t)}{I_0} = B_0 + \sum_{i=1}^{2} A_i \exp\left(-\frac{t}{\tau_i}\right)$$

where τ is the lifetime, t is the time, and I is the intensity. Intensities down to 1% of the initial intensities were included in the lifetime analysis, and the chi-square (χ^2) was in between 1.0−1.3.

Scanning Electron Microscopic (SEM) Measurements and Energy Dispersive X-ray Spectroscopy (EDS). The EDS analysis was done using a Bruker Quantax EDS System Link on the Hitachi S-4800 Field Emission Scanning Electron Microscope. The samples were gently crushed to make them uniform and placed on a sample holder covered with a sticky carbon tape. The electron paramagnetic resonance (EPR) spectrum was collected on a Bruker EMX instrument operating in the X-band (9.443 GHz) at 115 K. Raman spectra were collected by exciting the sample with a 632 nm from a He−Ne laser by Melles Griot. The solid sample was evenly spread over a clean glass slide. Each spectrum is an average of six scans with an objective of 50 X and collected over 30 s.

Fourier Transform Infrared (FTIR) Measurements. FTIR measurements were done using a Perkin-Elmer FTIR spectrometer 1000 machine. A KBr pellet was made by mixing dried KBr, and the sample was approximately in the ratio 10:1. All spectra were an average of four scans and recorded with a resolution of 2 cm^{-1}.

■ ASSOCIATED CONTENT

Supporting Information. Table S1 and Figures S1−S7. This material is available free of charge via the Internet at http://pubs.acs.org.

■ AUTHOR INFORMATION

Corresponding Author
*E-mail: fvv@uvic.ca.

■ REFERENCES

(1) Arakawa, Y. J. *Quantum Electron.* **2002**, *8*, 823.
(2) Denbaars, S. P. *Proc. IEEE* **1997**, *85*, 1740.
(3) Fasol, G. *Science* **1996**, *272*, 1751.
(4) Nakamura, S.; Fasol, G.; Pearton, S. *The Blue Laser Diode:The Complete Story*; Springer: Berlin, 1997.
(5) Nakamura, S.; Mukai, T.; Senoh, M. *Appl. Phys. Lett.* **1994**, *64*, 1687.

(6) Li, L.; Yang, Z.; Kong, J. Y.; Liu, J. L. *Appl. Phys. Lett.* **2009**, *95*, 232117.
(7) Steckl, A. J.; Heikenfeld, J. C.; Dong-Seon, L.; Garter, M. J.; Baker, C. C.; Yongqiang, W.; Jones, R. J. *Quantum Electron.* **2002**, *8*, 749.
(8) Tao, S.; Zhou, Y.; Lee, C.-S.; Zhang, X.; Lee, S.-T. *Chem. Mater.* **2010**, *22*, 2138.
(9) Light Emitting Diodes (LEDs) for General Illumination: An OIDA Technology Roadmap Updates2002. http://lighting.sandia.gov/lightingdocs/OIDA_SSL_LED_RoadmapFull.pdf.
(10) Grimsdale, A. C.; Leok Chan, K.; Martin, R. E.; Jokisz, P. G.; Holmes, A. B. *Chem. Rev.* **2009**, *109*, 897.
(11) Anthony, J. E. *Chem. Rev.* **2006**, *106*, 5028.
(12) Liu, J.; Pei, Q. *Macromolecules* **2010**, *43*, 9608.
(13) Von Ruden, A. L.; Cosimbescu, L.; Polikarpov, E.; Koech, P. K.; Swensen, J. S.; Wang, L.; Darsell, J. T.; Padmaperuma, A. B. *Chem. Mater.* **2010**, *22*, 5678.
(14) Wang, Y. Q.; Steckl, A. J. *Appl. Phys. Lett.* **2003**, *82*, 502.
(15) Lee, D. S.; Steckl, A. J. *Appl. Phys. Lett.* **2003**, *83*, 2094.
(16) Yang, K.-Y.; Oh, S.-C.; Cho, J.-Y.; Byeon, K.-J.; Lee, H. *J. Electrochem. Soc.* **2010**, *157*, H1067.
(17) Zhao, J. L.; Tan, S. T.; Iwan, S.; Sun, X. W.; Liu, W.; Chua, S. *J. Appl. Phys. Lett.* **2009**, *94*, 093506.
(18) Nakamura, A.; Ohashi, T.; Yamamoto, K.; Ishihara, J.; Aoki, T.; Temmyo, J.; Gotoh, H. *Appl. Phys. Lett.* **2007**, *90*, 093512.
(19) Guo, Z.; Zhang, H.; Zhao, D. X.; Liu, Y. C.; Yao, B.; Li, B. H.; Zhang, Z. Z.; Shen, D. Z. *Appl. Phys. Lett.* **2010**, *97*, 173508.
(20) Kudrawiec, R.; Nyk, M.; Syperek, M.; Podhorodecki, A.; Misiewicz, J.; Strek, W. *Appl. Phys. Lett.* **2006**, *88*, 181916.
(21) Mahalingam, V.; Tan, M.; Munusamy, P.; Gilroy, J. B.; Raudsepp, M.; vanVeggel, F. C. J. M. *Adv. Funct. Mater.* **2007**, *17*, 3462.
(22) Tan, M.; Munusamy, P.; Mahalingam, V.; van Veggel, F. C. J. M. *J. Am. Chem. Soc.* **2007**, *129*, 14122.
(23) Bagwe, R. P.; Yang, C.; Hilliard, L. R.; Tan, W. *Langmuir* **2004**, *20*, 8336.
(24) Dubois, L. H.; Zegarski, B. R. *J. Am. Chem. Soc.* **1993**, *115*, 1190.
(25) Zhang, J.; Jiang, F. *Chem. Phys.* **2003**, *289*, 243.
(26) Anedda, A.; Carbonaro, C. M.; Clemente, F.; Corpino, R.; Ricci, P. C. *J. Phys. Chem. B* **2004**, *109*, 1239.
(27) Mahalingam, V.; Bovero, E.; Munusamy, P.; van Veggel, F. C. J. M.; Wang, R.; Steckl, A. J. *J. Mater. Chem.* **2009**, *19*, 3889.
(28) Mahalingam, V.; Sudarsan, V.; Munusamy, P.; van Veggel, F. C. J. M.; Wang, R.; Steckl, A. J.; Raudsepp, M. *Small* **2008**, *4*, 105.
(29) Tan, M.; Mahalingam, V.; van Veggel, F. C. J. M. *Appl. Phys. Lett.* **2007**, *91*, 093132.
(30) van Krevel, J. W. H.; van Rutten, J. W. T.; Mandal, H.; Hintzen, H. T.; Metselaar, R. *J. Solid State Chem.* **2002**, *165*, 19.
(31) Schweizer, S.; Corradi, G.; Edgar, A.; Spaeth, J. M. *J. Phys. Condens. Mater.* **2001**, *13*, 2331.
(32) X-ray Powder Diffraction file JCPDS-ICDD (Joint Committee on Powder Diffraction Standard-International Centre for Diffraction Data) Swarthmore Swarthmore, PA, 1999.
(33) Cullity, B. D. Element of X-Ray Diffraction; Addison-Wesley Publishing Company Inc.: 1956.
(34) Williamson, G. K.; Hall, W. H. *Acta Metall.* **1953**, *1*, 22.
(35) Kuball, M.; Demangeot, F.; Frandon, J.; Renucci, M. A.; Massies, J.; Grandjean, N.; Aulombard, R. L.; Briot, O. *Appl. Phys. Lett.* **1998**, *73*, 960.
(36) Pan, G. Q.; Kordesch, M. E.; Van Patten, P. G. *Chem. Mater.* **2006**, *18*, 5392.
(37) Posset, U.; Lankers, M.; Kiefer, W.; Steins, H.; Schottner, G. *Appl. Spectrosc.* **1993**, *47*, 1600.
(38) Berrier, E.; Zoller, C.; Beclin, F.; Turrell, S.; Bouazaoui, M.; Capoen, B. *J. Phys. Chem. B* **2005**, *109*, 22799.
(39) Munusamy, P.; Mahalingam, V.; van Veggel, F. C. J. M. *Eur. J. Inorg. Chem.* **2008**, *21*, 3728.